



HAL
open science

Estimation of physical and physiological performances of blacklip pearl oyster larvae in view of DEB modeling and recruitment assessment

Nathanaël Sangare, Alain Lo-Yat, Gilles Le Moullac, Laure Pecquerie, Yoann Thomas, Benoit Beliaeff, Serge Andréfouët

► To cite this version:

Nathanaël Sangare, Alain Lo-Yat, Gilles Le Moullac, Laure Pecquerie, Yoann Thomas, et al.. Estimation of physical and physiological performances of blacklip pearl oyster larvae in view of DEB modeling and recruitment assessment. *Journal of Experimental Marine Biology and Ecology*, 2019, 512, pp.42-50. 10.1016/j.jembe.2018.12.008 . hal-02530665

HAL Id: hal-02530665

<https://hal.science/hal-02530665>

Submitted on 18 Jun 2020

HAL is a multi-disciplinary open access archive for the deposit and dissemination of scientific research documents, whether they are published or not. The documents may come from teaching and research institutions in France or abroad, or from public or private research centers.

L'archive ouverte pluridisciplinaire **HAL**, est destinée au dépôt et à la diffusion de documents scientifiques de niveau recherche, publiés ou non, émanant des établissements d'enseignement et de recherche français ou étrangers, des laboratoires publics ou privés.

Estimation of physical and physiological performances of blacklip pearl oyster larvae in view of DEB modeling and recruitment assessment

Sangare Nathanaël ^{1,*}, Lo-Yat Alain ¹, Le Moullac Gilles ¹, Pecquerie Laure ², Thomas Yoann ²,
Beliaeff Benoît ¹, Andréfouët Serge ³

¹ Ifremer, UMR 241 Environnement Insulaire Océanien (EIO), Labex Corail, Centre du Pacifique, BP 49, Vairao 98719, French Polynesia

² Laboratoire des Sciences de l'Environnement Marin (LEMAR), UMR 6539 IRD/UBO/Ifremer/CNRS, BP70, 29280 Plouzané, France

³ UMR9220 ENTROPIE, IRD, Université de la Réunion, CNRS, B.P.A5, 98848 Nouméa, New Caledonia

* Corresponding author : Nathanaël Sangare, email address : nathanael.sangare@ifremer.fr

Abstract :

In French Polynesia black pearl farming represents one of the dominant business sectors. However, it still entirely relies on unpredictable *Pinctada margaritifera* spat collection success, which is itself conditioned by larval development completion. To assess the relationship between larval development and recruitment success, we studied under controlled conditions the effect of food concentration on development, growth, ingestion rate, survival and metabolic rate at the larval stage. Larvae were exposed to four different phytoplankton densities (2,5; 7,5; 15 and 30 cell.µL⁻¹). Larvae survived equally all over the range of phytoplankton concentration with an average survival rate of 16% at the end of experiments. Food concentration significantly affected the larval physiology throughout its development from birth to metamorphosis. Growth and feeding were close to those reported by previous laboratory observations with young spat of 210 µm long obtained in 18 days of rearing at 28 °C for the highest food concentration. Differences in length at metamorphosis and cumulated energy ingested until settlement occurred according to trophic levels with a saturation threshold close to 0.0086 J.ind⁻¹. This level was reached at the food concentration of 15 cell.µL⁻¹. Larval development stages could be divided on the basis of the energy balance between feeding and respiration rates. An initial mixotrophic period with a lower and constant ingestion/respiration ratio over the first three days (from birth to D-veliger larva) was followed by an exotrophic phase characterized by a sharp increase in energy balance highly dependent of food concentration. Finally two sharp decreases of feeding rates were recorded during metamorphosis before umbonate and eyed stages. This study provided numerous new clues to establish a quasi-deterministic relationship between food condition and larval development. It highlights the major effect of food concentration and how energy intake through feeding as well as behavioral and physiological transitions can optimize larval development duration and minimize “the risky phase” of their life cycle. By taking into account the observed metabolic switches, the results provide a strong foundation for Dynamic Energy Budget model development and better description of the complex interactions between *P. margaritifera* physiology and environmental conditions.

Highlights

► *Pinctada margaritifera* larval phase is studied for DEB modeling. ► Food density highly impact physical traits of larvae such as age or size at settlement. ► Low food density is not lethal for pearl oyster larvae. ► Cumulated energy ingested until settlement differs according to trophic levels. ► Energetic balance reveals critical metabolic periods, especially during the metamorphosis phases.

Keywords : Bivalve larvae, *Pinctada margaritifera*, Physiology, Energetics, Dynamic energy budget theory, Pearl farming, Aquaculture

48 1. Introduction

49

50 In marine species, questions regarding the origin of recruitment variability first
51 appeared for fish populations (Hjort, 1926) before it was extended by Thorson (1950) to all
52 species with a planktotrophic larval phase. The link between larval stage, recruitment and
53 population dynamic is commonly described by the "supply-side ecology" hypothesis which
54 focus on the number of individuals surviving to recruit in habitats occupied by adults rather
55 than process causing death (Underwood and Fairweather, 1989; Grosberg and Levitan,
56 1992). Considered as a risky phase of the life cycle, the larval stage received a lot of
57 attention. Very early on, Hjort (1926) already made the assumption of an excess of mortality
58 when larvae start to feed by themselves. Then, the so-called optimal window theory (Cury
59 and Roy, 1989) linked spawning output and recruitment success through larval development
60 and environmental conditions. This theory emphasized that "match-mismatch" between the
61 presence of trophic resource and period of larval development can explain recruitment
62 variations for bivalves species (Olson, 1989; Menge *et al.*, 2009; Thomas *et al.*, 2011). The
63 lack of a quasi-deterministic relationship between spawning and recruitment continues to
64 confound attempts to fully understand and predict population dynamics. In the case of
65 bivalve larvae, growth and survival are determined by complex interactions between their
66 physiology and the environmental conditions (Widdows, 1991; Hofmann *et al.*, 2009) and
67 many studies have contributed to our understanding of how environmental variables
68 influence larval growth and development (Doroudi *et al.*, 1999a; 2000; Rico-Villa *et al.*, 2009).
69 Such studies were also instrumental in optimizing the hatcheries conditions for growth and
70 survival of bivalve larvae, for commercial cultivation.

71 In French Polynesia, pearl culture is based on the production of a single species: the
72 black-lipped pearl oyster (*Pinctada margaritifera*, Linnaeus, 1758) (Andréfouët *et al.*, 2012).
73 This activity has a major economic and social function since it employs about 1500 workers
74 and represents the second income of the country right behind tourism (ISPF, 2016). The

75 supply of juvenile oysters to the farms is largely dependent on the natural collection of larvae
76 on artificial substrates. This spat collection process takes place in 26 atolls and 4 islands (as
77 in 2017). For a given site, spat collection has proven to be very variable both spatially and
78 temporally, to the point that it may at time jeopardizes the steady supply of oysters to the
79 local demand. French Polynesian atoll lagoons have been described as stable and
80 homogeneous environments due to the low variations of water column characteristics in
81 comparison to temperate semi-enclosed system (Charpy *et al.*, 1997; Pouvreau *et al.*,
82 2000a). However, at the intra-lagoon scale, fluctuations in temperature and food
83 concentration occur in the water column (Fournier *et al.*, 2012; Pagano *et al.*, 2017). This
84 spatial and temporal heterogeneity can impact larval development, survival and dispersal
85 and ultimately the success of spat capture (Moran and Manahan, 2004 ; O'Connor *et al.*,
86 2007, Thomas *et al.*, 2016).

87 Since bivalve growth is directly linked to its environment (Southgate and Lucas,
88 2011), energetic models have been developed the last two decades to determine the role of
89 biotic and abiotic parameters on growth (Hofmann *et al.*, 2009; Pouvreau *et al.*, 2006; Powell
90 *et al.*, 2002). At the individual level, the Dynamic Energy Budget (DEB) theory (Kooijman,
91 2010) describes the processes of development, growth, maintenance, reproduction and
92 ageing for any kind of organism throughout its life cycle. A DEB model gives a representation
93 of the link between environment and physiological performances by describing the metabolic
94 rates, but it can also relate ecotoxicology to life traits for a given organism (Jager *et al.*, 2010;
95 Jager and Zimmer, 2012). Such models were successfully applied to well-studied species
96 such as *Crassostrea gigas*, an intensively cultivated bivalve (Rico-Villa *et al.*, 2010). For *P.*
97 *margaritifera*, temperature and food concentrations are considered to be the primary
98 environmental factors affecting the oyster physiological processes (Southgate and Lucas,
99 2011), but their influence on the metabolic rates during development remain poorly
100 documented.

101 To assess how environment and *P. margaritifera* physiology could be linked, Fournier
102 (2011) and Thomas *et al.* (2011) built two different DEB models for larvae and adult stage
103 respectively, that were partially calibrated based on parameters from *Crassostrea gigas*. The
104 larval DEB model has already been used and coupled with an hydrodynamic model to
105 investigate recruitment variation in space and time in an atoll lagoon (Thomas *et al.*, 2016).
106 Sensitivity analyses pointed out the major effect of the broodstock population structure, the
107 larval mortality rate and inter-individual growth variability. However, to date, an integrative
108 model for the full life cycle is still missing. A possible reason for this lack of integration may
109 be that all available data thus far on this species have been collected independently for a
110 variety of topics (genetic, evolutionary or comparative physiology and experimental
111 bioenergetics) that were not focused on informing a single model. To move forward, a DEB

112 model is currently in development to explicitly encapsulate all life stages into a single
113 bioenergetic model, and further integrate broodstock population dynamic and larval
114 performances (stage, mortality, fixation threshold) to the larval dispersal models initiated by
115 (Thomas *et al.*, 2016).

116 The accuracy of a DEB model for any given target species depends on the availability
117 of a set of parameters specific to the modeled species. The "covariation method" developed
118 by Lika *et al.*, (2011) provides specific sets of parameters which are estimated from standard
119 empirical datasets. The method has formalized 10 qualitative levels of parameterization,
120 which are directly linked to the nature of the empirical datasets on which the accuracy of the
121 parameters will depend. As the literature now provides a wide range of relevant
122 datasets(Doroudi *et al.*, 1999a; Doroudi *et al.*, 1999b; Doroudi and Southgate, 2003a, 2000;
123 Pouvreau *et al.*, 2000a, 2000b; Pouvreau and Prasil, 2001), *Pinctada margaritifera* currently
124 ranks at the fourth completeness level which refers to fits of growth (curve), age, length and
125 weight at birth and puberty at several food levels. This apparently low level is nevertheless
126 an achievement as well studied species such as *Magallana gigas* also reach the same level
127 4. The highest levels are reached when fluxes and balances for energy and elements (C, H,
128 O and N) are characterized at several body sizes and food levels, but these fluxes remain
129 very difficult to measure. Progress on rearing methods have contributed to enhance the
130 knowledge of the parameters necessary for the bioenergetic models for various species.
131 Ultimately, performances at larval stages, mortality rates, and fixation thresholds according to
132 environmental conditions could be used to enhance larval dispersal models, however,
133 specific ecophysiological data such as respiration rates remain rare for bivalve larvae
134 (Gerdes, 1983; Hamburger *et al.*, 1983) and nonexistent for *P. margaritifera* larvae.

135 In this context, this study assesses the effects of food concentrations on
136 development, growth, ingestion rate, survival and metabolic rate at the larval stage of *P.*
137 *margaritifera*. The new experimental results ultimately provides specific data useful for the
138 calibration of a DEB encompassing all life-stages of *P. margaritifera*. It also provides valuable
139 information on the links between larval growth, mortality and fixation thresholds that are
140 fundamental in the context of spat recruitment modeling.

141

142 **2. Material and Methods**

143

144 Experiments were conducted in hatchery at Ifremer facility (Vairao, Tahiti Island,
145 French Polynesia) from January to early February 2018 during the austral summer. Larvae
146 were reared from hatching to settlement over a range of four trophic levels.

147

148 *2.1 Production of larvae*

149

150 The spawning was obtained by thermal shock: seventy breeders (age: 6 years; mean
151 height \pm SD: 140 ± 10 mm) reared in the Vairao lagoon were progressively exposed from 26 to
152 18°C at 0.5°C per hour followed by a bath at 30°C . Four males and six females were
153 selected as genitors after microscopic observation of gametes morphology and sperm
154 motility. Fertilized eggs were stocked 24h in an aerated-seawater 500 L tank. Fertilization
155 and metamorphosis rates were measured then trochophore larvae were counted and
156 measured using a coulter counter (Beckman Multisizer 3) before being distributed in twelve
157 18 L breeding sieves at a density of 60 larvae. mL^{-1} .

158

159 *2.2 Experimental setup*

160

161 The larval rearing structure was made up of 12 cylinders of 25 L (30 cm diameter, 35
162 cm height). Then, $40\ \mu\text{m}$ mesh screens were fitted to the cylinders bottom to prevent loss of
163 larvae. Each rearing sieve was placed in another larger cylinder (40 cm diameter, 40 cm
164 height), equipped with an output to allow water discharge (Figure 1). The flow-through
165 system was set at a renewal rate of $50\%.\text{h}^{-1}$ ($220\ \text{mL}.\text{min}^{-1}$) of $1\ \mu\text{m}$ filtered and UV light
166 treated seawater. The water temperature was measured every hour with an accuracy of ± 0.1
167 $^{\circ}\text{C}$ using an iBcode 22L temperature sensor.

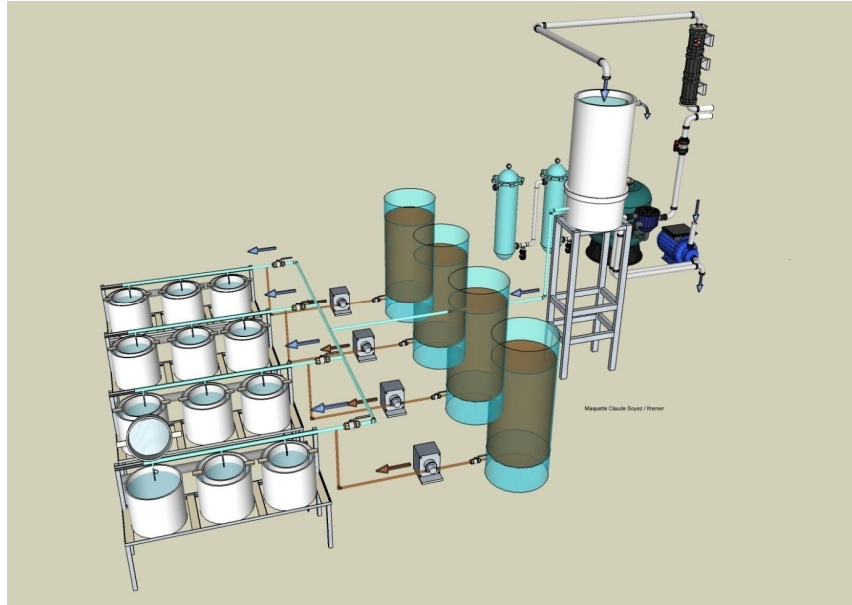
168

169 *2.2.1 Food conditions*

170

171 The 12 rearing sieves arranged in 4 rows corresponding to 4 trophic conditions
172 reproduced in triplicate (Figure 1) were supplied continuously with a mixture of cultured algae
173 in a 1:1 cells ratio of *Isochrysis lutea* ($Ti \approx 30\ \mu\text{m}^3$ volume diameter) and *Chaetoceros gracilis*
174 ($Cg \approx 60\ \mu\text{m}^3$). The algae diets were mixed at 4 different phytoplankton concentrations:
175 112.5 , 337.5 , 675 and $1350\ \mu\text{m}^3.\mu\text{L}^{-1}$ ($\approx 2,5$; $7,5$; 15 ; $30\ \text{cell}.\mu\text{L}^{-1}$ $TiCg$ equivalent diameter)
176 corresponding hereafter to 4 trophic levels respectively named C1, C2, C3 and C4.

177 According to Fournier *et al.* (2012), chlorophyll-a concentration is an accurate proxy
178 to quantify the available food for pearl oysters. The cultured algae concentrations relative to
179 the trophic levels number C1 and C2 were calibrated from available *in situ* measurements of
180 average fluorescence carried out during the 2017 austral winter (C1) and summer (C2) in the
181 lagoon of Ahe atoll (Thomas *et al.*, 2012, 2010). The trophic conditions C3 and C4 were
182 selected to follow the optimal breeding concentrations reported in the literature. According to
183 Doroudi and Southgate (2000), these concentrations represent the optimum ratio for larval
184 rearing and development ratio for the first 8 days of larval phase.



185

186 **Figure 1 Experimental design used to allow continuous algae supply at the four concentrations, in a flow-**
 187 **through larval rearing system.**

188

189 *2.3 Quantification and analysis of larval development*

190

191 The physical and physiological performances of the differently fed oysters were
 192 measured with similar time step until fixation for each trophic condition. One sample per tank
 193 was taken at days: 1; 3; 4; 5; 6; 8; 11; 13; 16; 18; 23; 27; 31 and 35.

194 Averages growth and mortality were obtained by measuring larval individual size (\pm
 195 0.1 μm) and larval density. These measurements were carried out using the coulter counter
 196 and considering larvae as spherical item with 100 mL samples taken from each of the 12
 197 rearing sieves after homogenization.

198 The average individual respiration rate was obtained for each trophic level from a
 199 sample of 150 000 larvae. Individuals were sifted on a 40 μm mesh in order to eliminate
 200 microalgae and then collected in a hermetic DBO Winkler bottle of 300 mL. The
 201 concentration of dissolved oxygen was measured with an optode (WTW inoLab® Multi 9310
 202 IDS) and recorded every minute during 70 minutes. The individual hourly consumption was
 203 computed from i) the decrease of dissolved oxygen concentration and ii) the count of larvae,
 204 achieved with the coulter counter corrected by a coefficient of percentage of living
 205 individuals, which was estimated by counting a sub-sample of 300 individuals under a
 206 microscope.

207 The feeding rate per larva was obtained by sampling twice a day the enriched filtered
 208 sea water at the inlet and outlet of each larval rearing cylinder (Figure 1). Thus, after
 209 controlling that the algae sedimentation rate was negligible in a reference sieve, microalgae
 210 concentrations were obtained from 20 mL samples analyzed with the coulter counter. The

211 difference of numbers of particles between the in- and outlet was calculated and divided by
212 the larval density. Then results were divided by the mean larval size to express feeding rate
213 in $\mu\text{m}^3 \cdot \mu\text{m}^{-1} \cdot \text{h}^{-1}$.

214 The age at settlement was assumed to be when at least 50% of the individuals were
215 fixed on the sieves sides. For each sieve, the percentage of fixation was obtained from the
216 ratio of swimming larvae density over total oyster density.

217 During oyster's development, the energetic balance calculation followed the scope for
218 growth (SFG) concept (Bayne, 1976), with the exception of the assimilation efficiency
219 coefficient since faecation and pseudofaecation were not measured. Thereby, the algae
220 ingested and respiration were converted into energy values and the difference between both
221 yielded the energetic balance. We used as conversion factors 3.81×10^{-9} J per μm^{-3} of algae
222 mixture (González-Araya *et al.*, 2011; Yukihiro *et al.*, 2000) and 14.1 J for 1 mg O_2 (Bayne
223 and Newell, 1983; Gnaiger, 1983). In order to smooth the graphical representation of the
224 results, linear mixed models (see below) fitted on observation data were used to estimate the
225 missing values between observations.

226 Finally, the cumulated ingested energy at metamorphosis was estimated as the
227 energetic value of the sum of the daily average number of cells ingested per individual until
228 settlement. Despite the fact that algae consumption was recorded daily for each tanks, the
229 density of larvae per tank was not continuously measured. Hence, linear mixed model results
230 were used to fill the missing larval density data.

231

232 2.3.1 Statistical analysis

233

234 All analyses were performed with the software R v.3.4.1 (R Development Core Team,
235 2012). Considering our experimental set up; in order to assess the effects of the four different
236 trophic levels on the evolution of size, mortality and length-normalized respiration and
237 feeding rates as repeated measurement over time, mixed effects analyses using the 'lmer'
238 function of R package 'lme4' (Bates *et al.*, 2017) were performed. Relationships were tested
239 using random intercept and slope linear mixed models. The fixed effects feed ration was
240 considered as a factor and time was a continuous numeric variable. The variable tank was
241 set as a random factor. The 'anova' function (default) in the 'car' package (Fox *et al.*, 2012)
242 was used to compute the significance tests and provide *p values*. In addition, a one-way
243 ANOVA was performed to investigate the effect of food concentration on the age at
244 settlement.

245 Before the mixed effects analyses, data were Box-Cox transformed to improve
246 normality. Model predictions were back transformed to plot the results using the R packages
247 'MASS', 'car' and 'ggplot2' (Fox *et al.*, 2012; Ripley *et al.*, 2013; Wickham, 2010).

248 After mixed effects analyses, pairwise comparison by post-hoc Tukey analysis were
249 performed thanks to the 'multcomp' and 'lsmeans' packages (Hothorn *et al.*, 2017; Lenth,
250 2016) to determine how trophic levels differed from each other.

251 The outputs were printed thanks to the 'tab_model' function of the 'sjPlot' package
252 (Lüdecke, 2015). In any case, the normality of the residuals was checked (Shapiro–Wilk test)
253 and the homoscedasticity of the variance of errors was visually assessed.

254 Note that to focus the results on the larval stage, all mixed effects analyses were
255 strictly applied on data recorded before settlement. Finally to avoid time vector length issues
256 related to dissimilar ages at settlement, break points over time were visually assessed.

257

258 **3. Results**

259

260 *3.1 Temperature profile*

261

262 During the experiment, the recorded mean temperature was 28.1°C with daily
263 fluctuations of up to 0.5 °C within 24h. A general decrease of daily mean temperature
264 occurred from 28.9 to 27.6 °C between the first and the last day of rearing (see
265 Supplementary Figure 1). A maximum of 29.6 °C and a minimum of 26.7 °C were recorded.
266 They appeared the fifth and 25th day of the experiment respectively. No difference in
267 temperature was measured between the different rearing tanks.

268

269 *3.2 Effects of food concentration*

270

271 Food condition, time and their interaction had significant effects on larval
272 development variables (*p-values* < 0.05) for each statistical test performed, with the
273 exception of the mortality rate for which only time was significant (Table 1).

274 **Table 1 Summary of random intercept and slope linear mixed models fitted on larval performance**
 275 **measurements recorded from birth until settlement. *p*-values numbers marked in bold indicate numbers**
 276 **that are significant on the 90% confidence limit.**

Predictors	Growth			Respiration rate			Feeding rate			Mortality rate		
	Estimates	CI	<i>p</i>	Estimates	CI	<i>p</i>	Estimates	CI	<i>p</i>	Estimates	CI	<i>p</i>
(Intercept)	0.99109	0.99076 – 0.99143	<0.001	-7.76069	-7.95216 – -7.56921	<0.001	0.92428	-0.09900 – 1.94755	0.105	-6.54297	-30.17951 – 17.09357	0.592
Time	0.00030	0.00028 – 0.00033	<0.001	0.10847	0.09867 – 0.11828	<0.001	0.14802	0.11158 – 0.18447	<0.001	9.26121	8.12855 – 10.39387	<0.001
Food condition 2	-0.00005	-0.00055 – 0.00046	0.862	0.43380	0.13985 – 0.72776	0.005	1.94855	0.48791 – 3.40919	0.024	19.16938	-14.25773 – 52.59649	0.272
Food condition 3	-0.00008	-0.00062 – 0.00045	0.759	0.37742	0.06804 – 0.68679	0.020	2.50133	1.02023 – 3.98242	0.006	36.30233	2.87521 – 69.72944	0.044
Food condition 4	-0.00108	-0.00161 – -0.00055	<0.001	0.23626	-0.07311 – 0.54564	0.139	1.12883	-0.35227 – 2.60992	0.161	49.13853	15.71141 – 82.56564	0.008
Time:Food.condition2	0.00009	0.00005 – 0.00013	<0.001	0.02688	0.00911 – 0.04464	0.004	0.01557	-0.04297 – 0.07410	0.603	-0.58612	-2.18795 – 1.01571	0.474
Time:Food.condition3	0.00016	0.00011 – 0.00021	<0.001	0.08092	0.05967 – 0.10216	<0.001	0.18553	0.11554 – 0.25551	<0.001	0.10257	-1.49925 – 1.70440	0.900
Time:Food.condition4	0.00024	0.00019 – 0.00029	<0.001	0.10102	0.07977 – 0.12227	<0.001	0.27397	0.20398 – 0.34395	<0.001	-1.10078	-2.70260 – 0.50105	0.180
Random Effects												
σ^2	0.00			0.05			0.78			999.23		
τ_{00}	0.00 Tank			0.00 Tank			0.63 Tank			182.56 Tank		
ICC	0.00 Tank			0.00 Tank			0.44 Tank			0.15 Tank		
Observations	144			72			129			180		
Marginal R ² / Conditional R ²	NA			NA			0.765 / 0.869			0.824 / 0.851		

278

279 The post-hoc Tukey analysis exhibited different levels of significance depending on
 280 the tested physiological performance and the pair of tested trophic levels (Table 2).

281

282 **Table 2 Simultaneous tests for general linear hypotheses with Tukey contrasts multiple comparisons of**
 283 **means, fitted on linear mixed models of food concentration and time effect on larval size, respiration,**
 284 **feeding and mortality and the ANOVA relating the food concentration effect on the age at settlement. *p*-**
 285 **values numbers marked in bold indicate numbers that are significant on the 90% confidence limit.**

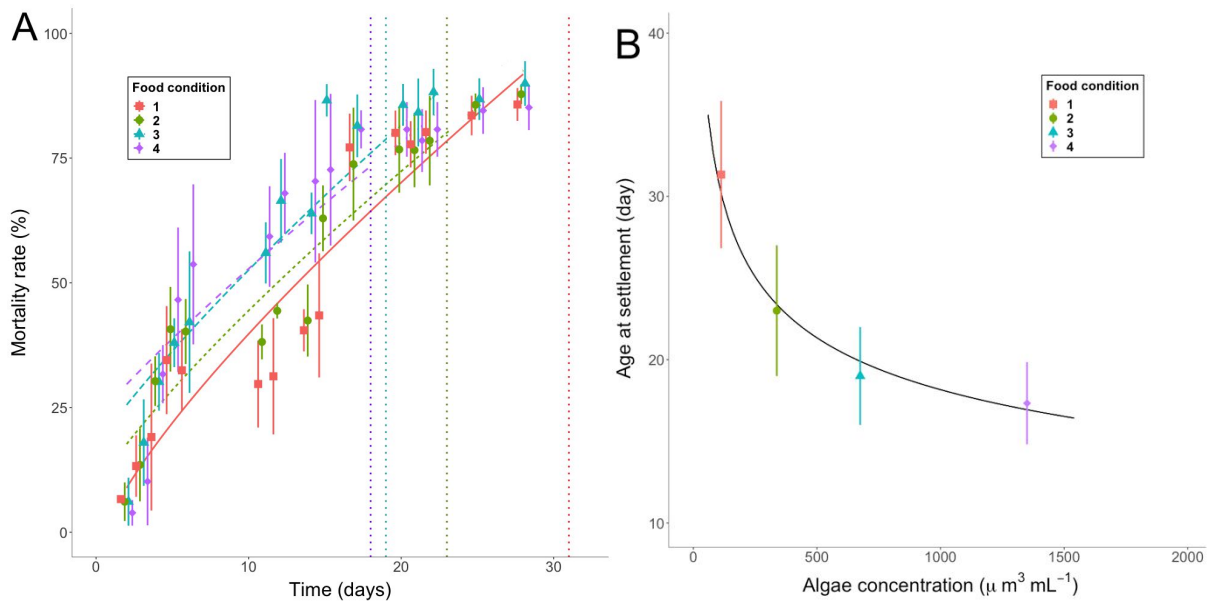
Physiological performance	Compared conditions	C1 - C2	C1 - C3	C1 - C4	C2 - C3	C2 - C4	C3 - C4
Growth	Estimate	-0.0007438	-0.0013655	-0.0010864	-0.0006217	-0.0003427	0.0002790
	Pr(> t)	0.00594	< 0.001	<0.001	0.02419	0.26089	0.44649
Respiration rate	Estimate	-0.80558	-1.49674	-1.63372	-0.69117	-0.82814	-0.13698
	Pr(> t)	< 0.001	<0.001	< 0.001	<0.001	<0.001	0.441
Feeding rate	Estimate	-2.0952	-4.2487	-3.7092	-2.1536	-1.6141	0.5395
	Pr(> t)	0.06244	0.00107	0.00287	0.05667	0.16898	0.86254
Mortality	Estimate	-11.16	-34.09	-37.70	-26.55	-22.93	3.61
	Pr(> t)	0.822	0.110	0.074	0.244	0.348	0.992
Age at settlement	Estimate	-0.3813	-0.6089	-0.7167	-0.2276	-0.3355	-0.1078
	Pr(> t)	0.13909	0.01779	0.00721	0.49144	0.20906	0.89429

286

287

288 3.2.1 Survival and settlement

289



290

291 **Figure 2 (A) Evolution of the percentage of dead oysters across time under different feeding conditions.**
292 **(B) Mean age at settlement according to food concentration. The continuous curves are predictions from**
293 **the models that were fitted to the observations (symbols), with the standard errors (vertical lines). The**
294 **vertical dotted lines mark the age at settlement for each trophic level.**

295

296 Regardless of the time dynamic, larval survival was low on day 22, with mortality \approx
297 78% corresponding to a drop from 60 to 10 ind.mL⁻¹ (Figure 2A) and no significant difference
298 between conditions (ANOVA, $p = 0.201$). During the rearing, different dynamics occurred
299 between trophic levels. On day 12, larval mortality ranged from 28% to 43% at the lowest
300 food concentrations (C1 and C2) and from 64% to 68% for the highest food concentration C3
301 and C4, with significant differences between contrasted food conditions C1 and C4 (Table 2).

302

303 The age at settlement increased exponentially with the diminution of the food
304 concentration. From the lowest to the highest trophic level, the age at settlement was 31, 23,
305 19 and 18 respectively (Figure 2B), with significant differences only between the lowest and
the two highest food conditions (Table 2).

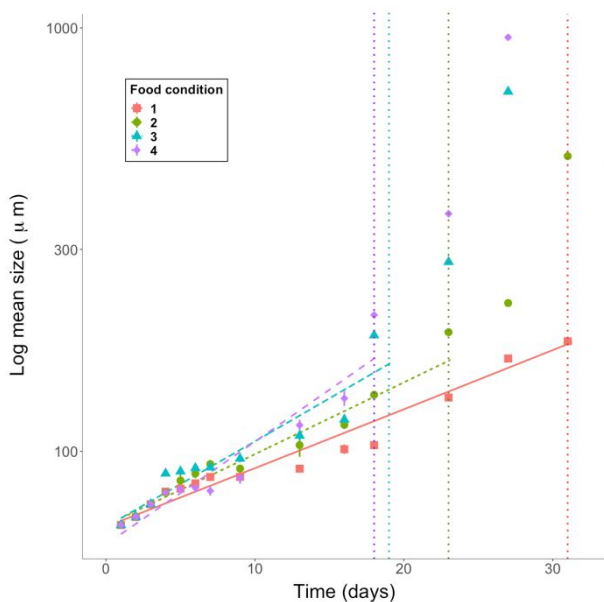
306

307 3.2.2 Growth

308

309 Significant differences in growth rate between food levels were recorded mainly from
310 day-12. Differences were significant between diets, excepted for the comparison of the
311 conditions C2 versus C4 and C3 versus C4 (Table 2). In addition to growth speed variations
312 related to the food concentration, the size at settlement varied with the diet, reaching an
313 average size of 210, 200, 190, and 180 μm at the trophic levels C4, C3, C2 and C1,
314 respectively. After settlement, growth increased sharply. For instance, for the highest food

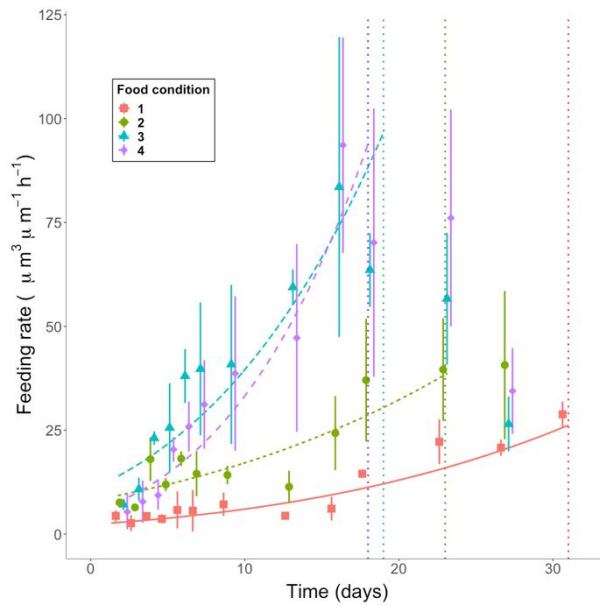
315 level C4, the size went from 67 to 210 μm during the first 18 days and from 210 to 950 μm
316 between the following 9 days (Figure 3). Despite the apparent reciprocity between growth
317 and food concentration, it appeared that larvae grew faster within the first 8 days at C3 (675
318 $\mu\text{m}^3 \cdot \mu\text{l}^{-1}$) than C4 (1350 $\mu\text{m}^3 \cdot \mu\text{l}^{-1}$). This trend changed when larvae reached a mean size of
319 100 μm after which the fastest growth was recorded for the highest trophic level.
320



321
322 **Figure 3 Oyster growth (log scale) over time for the different food conditions. The continuous curves**
323 **show predictions from the linear mixed models that were fitted to the observations (symbols) with the**
324 **standard error (vertical lines), for each food condition. Vertical dotted lines represent the age at**
325 **settlement. The values after settlement are not taken into account in the models.**
326

327 3.2.3 Feeding rate

328



329

330 **Figure 4 Oyster algae consumption per hour as a function of age for different food conditions. The**
331 **feeding rate is scaled by unit of length. The continuous curves show predictions from the linear mixed**
332 **models that were fitted to the observations (symbols) with the standard error (vertical lines). Vertical**
333 **dotted lines represent the age at settlement for each trophic level. The values after settlement are not**
334 **taken into account in the models.**

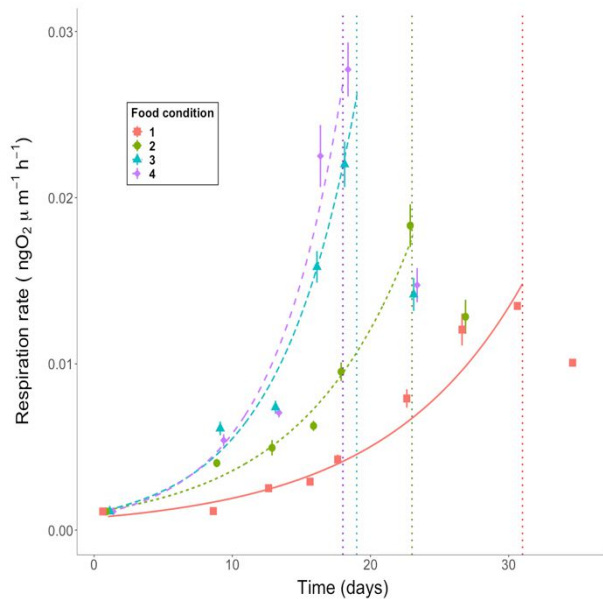
335

336 Feeding rate was highly dependent on food concentration and could be described
337 visually by three regimes. For high food concentration, standard deviations were important
338 and statistically no significant differences were reported between the trophic levels C3 versus
339 C4 and C2 versus C4 (Table 2). At low food concentration, the increased consumption was
340 closely related to phytoplankton density. At high food concentration, feeding rate was higher
341 at $675 \mu\text{m}^3 \cdot \mu\text{l}^{-1}$ (C3) than $1350 \mu\text{m}^3 \cdot \mu\text{l}^{-1}$ (C4) within the first 8 days of the rearing then this
342 trend switched and the feeding rate increased faster at high food concentration. A microalgae
343 uptake decrease corresponding to settlement was thereafter observed when the feeding rate
344 was length-normalized (Figure 4) but this trend did not occur if the feeding was expressed as
345 hourly uptake per individual (not shown). Moreover, independently of the size, a slight
346 decrease in the feeding rate also appeared during the transition in the umbo and eyed
347 stages, respectively close to days 7/8 and 17/19 for conditions C4 and C3. At low food level
348 (conditions C1 and C2) this trend is less obvious for the umbo stage but clearly appeared few
349 days before the metamorphosis of eyed larvae. Finally, a generalized drop of food intake
350 clearly appeared on day 15 which matched the main peak of mortality.

351

352 3.2.4 Metabolic rate

353



354

355

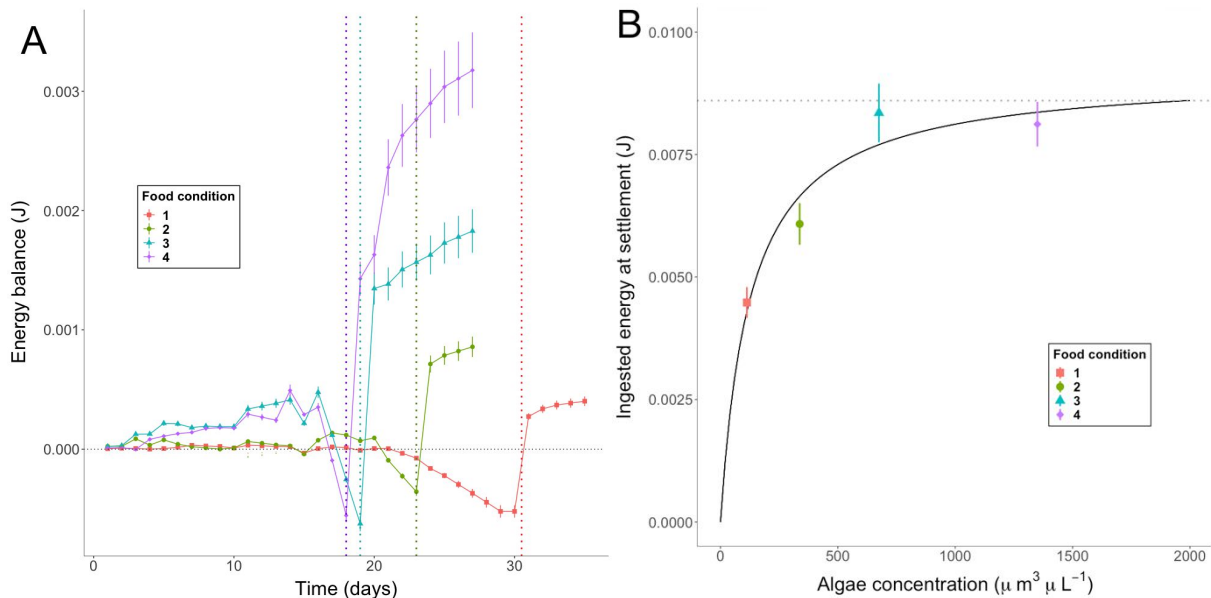
356 **Figure 5** Oyster respiration rate according to their age under different feeding conditions. The respiration
 357 rate is scaled by unit of length. The continuous curves show predictions from the linear mixed models
 358 that were fitted to the observations (symbols) with the standard error (vertical lines). Vertical dotted lines
 359 represent the age at settlement for each trophic level. The values after settlement are not taken into
 360 account in the models.

361

362 Over time, the length-normalized respiration varied significantly between trophic
 363 levels except for the food concentrations C3 and C4 (Figure 5). There was an exponential
 364 increase in respiration rates with time with a marked decrease in metabolic rate after fixation
 365 of the eyed larvae. This decrease in breathing was apparent when the respiration was not
 366 length normalized and coincided with the cessation of the active search for food. Indeed, this
 367 is the moment when individuals stopped swimming and attached themselves to a substrate
 368 from which they started filtering the surrounding water.

369 During the first 3 days, the balance between energy consumed and ingested was
 370 close to 0 ($\approx 4 \times 10^{-6} \text{ J.day}^{-1}$) (Figure 6A). Then, it slowly increased at food concentrations C3
 371 and C4 while it remained in a 2×10^{-5} to $1.3 \times 10^{-4} \text{ J.day}^{-1}$ range during the entire larval phase
 372 at low food concentrations (C1 and C2). Similar to the feeding rate dynamic, drops in energy
 373 balance occurred at time of the switches to the umbo and eyed stages as well as during
 374 major mortality events. This resulted in possible peak or plateau of negative energetic
 375 balance. The extent of these periods depended on the time required by the whole batch to
 376 fully move toward the next larval development stage.

377 The cumulated ingested energy at settlement increased with food concentration but a
 378 saturation threshold close to 0.0086 J.ind⁻¹ is observed at C3 concentration (675 μm³ μl⁻¹ ≈
 379 15 cell μL⁻¹ TiCg equivalent diameter) (Figure 6B).
 380



381
 382 **Figure 6. (A) Energy balance between food intake and respiration over time, vertical dotted lines**
 383 **represent the age at settlement for each trophic level. (B) Cumulated energy consumed at metamorphosis**
 384 **against food concentration. The continuous curve shows a Holling type II functional response fitted**
 385 **against the observations. Vertical bars are standard errors (A & B).**
 386

387 4. Discussion

388

389 The present study aimed to assess, in view of DEB modeling, the effect of food
 390 concentration on *Pinctada margaritifera* larval performances and development efficiency.
 391 This study also incidentally identified metabolic traits that can be explained by behavioral and
 392 physiological changes at key moment of larval development. These new observations are
 393 fundamental in view of recruitment modelling.

394

395 4.1. Effects of food density on larval development

396

397 A close relationship between performances and feeding regime was demonstrated
 398 during larval development within the range of tested food densities (Table 1). During the
 399 larval phase, the amount of food consumed is an essential factor in successful settlement as
 400 larvae must accumulate sufficient reserves to meet the energy demands required during
 401 metamorphosis (Strugnell and Southgate, 2003). The dynamic of the cumulated energy
 402 ingested at settlement was in accordance with previous studies that reported differences in

403 post settlement size and biochemical composition of bivalves raised at different trophic levels
404 (Holland and Spencer, 1973; Pechenik, 1990). These physical dissimilarities were closely
405 related to the different ages at settlement that ranged in our case from 18 to 31 days. Our
406 observations substantially differed from those observed by Doroudi and Southgate, (2003a)
407 for the maximum age at settlement who reported settlement from 16 to 21 days in laboratory
408 at 28.1 °C, but they agree with the 29 days reported by Thomas *et al.*, (2011) during *in situ*
409 larval survey, which corresponds to our low food level conditions.

410 Here, larval growth was directly correlated with food density up to 20 cells μL^{-1} and
411 the optimal algal ration remained within a range of 4.5–11.5 and 15–32 cells μL^{-1} for 7- and
412 20-day-old larvae respectively. These results are in agreement with Doroudi *et al.*, (1999b)
413 and Doroudi and Southgate, (2000). Similarly, the recorded feeding rates per individual were
414 in the range of those reported by Doroudi *et al.*, (2003b): 8.7 to 165 cells h^{-1} larvae $^{-1}$
415 respectively for larvae with shell length of 89 and 188 μm . Here feeding rates were highly
416 dependent of the shell length and varied from 11.4 to 279.1 cells h^{-1} larvae $^{-1}$ from birth to
417 settlement for well-fed larvae.

418 The respiration rates measured here (Figure 5) add to the rather shortlist available
419 data reported for bivalve larvae. Our range of respiration rates was consistent with the rates
420 measured for well fed *Crassostrea gigas* larvae (Gerdes, 1983) which rank from 0.4 to 6.1
421 $\text{nI}_2\text{O}_2 \text{ h}^{-1}$ larva $^{-1}$. Here, during larval development, *P. margaritifera* larvae respiration rate
422 increased from 0.1 to 4.5 $\text{ngO}_2 \text{ h}^{-1}$ larva $^{-1}$. The DEB theory (Kooijman, 2010) itself does not
423 use respiration rate as a primary variable, however, this information can be used to test in
424 fine the model parameters accuracy.

425 The energetic balance calculation, with the exception of the assimilation efficiency
426 coefficient, was based on the scope for growth (SFG) concept (Bayne, 1976) and the
427 respiration-energy equivalent is directly subtracted from the energy derived from assimilated
428 food. The energy left remains available for growth. Such calculations remain inexistent for
429 bivalve larvae in the literature so far, respiration rates were measured over short periods and
430 the interpolation of missing value may not be suitable for such calculation so these data have
431 to be used meagerly. Moreover, discrepancies can arise because subtracting from the
432 ingested food energy the energy-equivalent from respiration is only an approximation as
433 respiration rates should compensate for both metabolic and growth costs (Kooijman, 2010).

434 The survival rates obtained here partially also agreed with the early studies (Doroudi
435 *et al.*, 1999b; Doroudi and Southgate, 2000). We observed high mortality rates up to 7.5 cells
436 μL^{-1} ($\approx 337.5 \mu\text{m}^3 \mu\text{L}^{-1}$) at day 12 but no significant differences occurred between the four
437 tested trophic levels within 22 days of rearing. Moreover, mortality showed important
438 standard deviation corresponding to large differences of mortality episode within the
439 replicates of one trophic level. As suggested by Asmani *et al.* (2017), mortalities may be due

440 to increased microbial activity or reduced water quality associated with unconsumed food
441 decomposition and larvae excretion. The synchronicity between mortality and feeding
442 decreases suggests that mortality episodes may relies on exogenous factors such as
443 microbial infection accompanied by a non-feeding behavior

444

445 *4.2 Influence of behavioral and ecological breaks*

446

447 As reported in the literature, development and metamorphosis were closely related to
448 the trophic levels, nonetheless this study suggests several behavioral and physiological
449 particularities, or breaks, that occurred sooner or later depending on food concentrations.
450 This is apparent here with the decrease of food consumption before settlement, confirming
451 that metamorphosis is a metabolic singularity within larval development. As for embryonic
452 development, metamorphosis strictly rely on reserve storage, for which environmental food
453 concentration and reserve accumulation are required for an optimized larval period duration
454 (Doroudi and Southgate, 2003). It appeared that reserve accumulation was directly linked to
455 food concentration, and as a consequence, the eyed stage could occur at different ages and
456 sizes depending on food availability. Therefore, well fed larvae will settle earlier and at a
457 bigger size than underfed larvae, and with differences of accumulated total energy ingested
458 until settlement. This energetic pattern agreed with the assumptions described by the DEB
459 theory (Kooijman, 2010) and the influence of available energy on delayed metamorphosis
460 (Doroudi and Southgate, 2003; Holland and Spencer, 1973; Pechenik, 1990) It can be stated
461 that larval development for a given temperature relies primarily in the available energetic flux,
462 and thus food quality/quantity, rather than genetic or other exogenous factors. Note that
463 temperature may delay metamorphosis but this is also dependent on the energetic flow since
464 no difference in size and cumulated ingested energy at settlement occurred for bivalve larvae
465 reared at different temperatures but with similar food density (Doroudi *et al.*, 1999a; Rico-
466 Villa *et al.*, 2009).

467 Settlement marks the end of the planktonic phase and comes with profound
468 physiological changes. The post settlement metabolic rate drop can be related to the
469 behavioral and morphological changes undergone by the pediveliger larvae. Indeed, when
470 the competences for metamorphosis are reached, pediveliger larvae enhance their crawling
471 behavior using their foot to find a suitable substrate to settle on, hence reducing their filtration
472 activity (Cole, 1937). Movement and feeding are also inhibited because the velum is
473 absorbed and replaced by the gills (Cole, 1938) and further developments need to rely on
474 previously accumulated endogenous reserves (Holland and Spencer, 1973). Once the larvae
475 are fixed, these drastic anatomic changes may cause the decrease in respiration rate
476 observed at the end of the larval life. In other words, whilst the growth accelerates, the

477 respiration rate decreases at the same time. In fact, by stopping swimming, the part of the
478 energy allowed to growth can increase. This suggests that settlement allow oysters reducing
479 their global metabolic activity.

480 Breaks in metabolic rates are not visible only at the end of the larval stage. During the
481 first 2 days, while shell length was increasing, feeding rates were relatively low and
482 independent from the food concentration. This observation suggests that the development of
483 newly released *P. margaritifera* larvae relies not only on exogenous source of food but also
484 on maternal reserves and so on initial gamete quality. This is in agreement with Ehteshami *et*
485 *al.*, (2011) who showed that diet during broodstock conditioning was influencing greatly
486 gonad composition, reproductive output and embryonic development. This mixotrophic phase
487 could therefore explain the low ingestion activity observed in the first days.

488 From day 2 to day 8, feeding was correlated with microalgae concentration except at
489 the 675 (C3) and 1350 (C4) $\mu\text{m}^3 \mu\text{L}^{-1}$ concentrations, where growth and respiration rate of
490 larvae in C3 condition showed higher performance than in C4. This result agreed with
491 previous studies (Doroudi *et al.*, 1999a; Doroudi and Southgate, 2000) and could be
492 explained by a temporary increase of microbial activity due to the decomposition of
493 unconsumed algae. This may lower the larvae performances. This hypothesis is confirmed
494 by the fact that at the same period mortality increased with the rise of phytoplankton
495 concentration. Nevertheless, after 8 days of rearing, when larvae reached a length up to 100
496 μm , growth and feeding rates correlated with food density again.

497 Finally, after settlement, the decrease of the length-normalized feeding rate may just
498 come from the increasing growth rather than behavioral or morphological changes, since the
499 feeding rate per individual increases continuously. This behavior may also be reinforced by
500 some physiological adaptation that allows oysters to support easily low food conditions that
501 they cannot offset if they actively research food in the water column.

502 We suggest, as future perspectives, that all these behavioral patterns should be
503 investigated in details by conducting similar experiences focusing on the oyster response to
504 environmental possible constraint by measuring metabolic changes at settlement and
505 minimal reserve dynamic. In addition, weight measurements and vibrio activity control should
506 be added to assess mortality causes and metamorphosis reserve requirements.

507

508 *4.3 Implications for spat collection*

509

510 The behavioral and physiological patterns observed here provide new clues to
511 interpret spat collecting success in tropical atoll lagoons, like it is commonly practiced in
512 French Polynesia by the pearl farming industry. Commonly described as environmentally
513 homogenous, the semi enclosed atoll lagoons in fact present relatively low temperature

514 variations (3 °C during the year), but not negligible food concentration variations in space
515 and time (Thomas *et al.*, 2016, 2010). Food variability is the main driving factor for larval
516 development success. First it affects broodstock gonad composition and reproductive output
517 that sets egg size and quality (Ehteshami *et al.*, 2011); then it determines the success of the
518 mixotrophic phase, the period of larval development (Rico-Villa *et al.*, 2009) and the size at
519 settlement. Low food condition is not lethal for larvae but highly impact growth speed, which
520 delays settlement and ultimately increases *in situ* mortality rate by predation (Marshall *et al.*,
521 2009). Furthermore, after settlement the individual size might represent a competitive
522 advantage in term of accessibility to the trophic resource. Spat survival may also depends on
523 its size at settlement and its ability to redirect the energy allowed to the swim for the benefit
524 of the growth speed. Thus, spat collecting effectiveness depends on a suite of processes that
525 can be easily affected by a disruption of food supply as our experiments suggest. It also
526 indirectly confirms pearl farmers empirical observations who have reported better spat
527 collecting during the austral summer, a period generally with more favorable environmental
528 conditions with suitable food concentrations.

529

530 4.4 Implications for DEB modeling

531

532 In this study, the two trophic levels C1 and C2 were calibrated to match extremes *in*
533 *situ* food conditions reported from the field (in atoll lagoons). The results matched field data
534 recorded by Thomas *et al.*, (2011) with a larval size of 180 µm reached in 20 days at 29.4 °C
535 against 190 µm in 23 days at 28.1 (C2) in this laboratory experiment. Despite expected
536 differences in term of food quality between field and laboratory, chlorophyll-a is confirmed as
537 a good proxy to model the growth of pearl oyster larvae. Furthermore, this contribution
538 creates a tangible basis for a future *P. margaritifera* DEB model able to represent the full life
539 cycle of the black lipped pearl oyster, with better parameterization of the larval stages. The
540 DEB will be much more robust after detailing, like here, physiological processes directly
541 relevant for Dynamic Energy Budget model parameterization (e.g., through the maximum
542 surface-area-specific ingestion rate or the half saturation coefficient) and by providing data
543 sets to accurately estimate values for the parameters controlling processes such as growth
544 and respiration rate.

545

546 5. Conclusion

547

548 This work highlighted the effect of food concentration on the processes related to
549 pearl oyster population recruitment success. Supported by previous laboratory observations,
550 it demonstrates how energy intake through feeding as well as behavioral and physiological

551 transitions allow optimizing the larval development duration and minimizing "the risky phase"
552 of their life cycle. This study provided numerous new clues to establish a quasi-deterministic
553 relationship between temperature and food condition in one hand and larval development
554 and recruitment success in the other hand. By taking into account the metabolic switches
555 that we could characterize, this study provides a strong foundation for DEB modeling
556 development and for a better description of the complex interactions between *P.*
557 *margaritifera* physiology and environmental conditions.

558

559 **Acknowledgements**

560

561 This study was co-funded by the Institut français de recherche pour l'exploitation de la
562 mer (IFREMER) and the Direction des Ressources Marines et Minières de Polynésie
563 française (DRMM). Support was also provided through the ANR-16-CE32-0004 MANA
564 (Management of Atolls) project. The authors thank the IFREMER and DRMM teams who
565 participated in the experiments conducted at Vairao and thank Elke Zimmer for her helpful
566 comments on experimental design, Quentin Schull for his conceptual and technical support
567 in R code development and Claude Soyez for drawing the Figure 1.

568

569 **References**

570

- 571 Andréfouët, S., Charpy, L., Lo-Yat, A., Lo, C., 2012. Recent research for pearl oyster aquaculture
572 management in French Polynesia.
- 573 Asmani, K., Petton, B., Le Grand, J., Mounier, J., Robert, R., Nicolas, J.-L., 2017. Determination of
574 stocking density limits for *Crassostrea gigas* larvae reared in flow-through and recirculating
575 aquaculture systems and interaction between larval density and biofilm formation. *Aquat. Living*
576 *Resour.* 30, 29.
- 577 Bates, D., Bolker, B., Walker, S., Singmann, H., Dai, B., Scheipl, F., Grothendiech, G., Green, P.,
578 2017. Package 'lme4.' <https://doi.org/10.2307/2533043>>
- 579 Bayne, B.L., 1976. *Marine Mussels: Their Ecology and Physiology*. Cambridge University Press.
- 580 Bayne, B.L., Newell, R.C., 1983. Physiological energetics of marine molluscs, in: *The Mollusca*,
581 Volume 4. Elsevier, pp. 407–515.
- 582 Charpy, L., Dufour, P., Garcia, N., 1997. Particulate organic matter in sixteen Tuamotu atoll lagoons
583 (French Polynesia). *Mar. Ecol. Prog. Ser.* 55–65.
- 584 Cole, H.A., 1938. The fate of the larval organs in the metamorphosis of *Ostrea edulis*. *J. Mar. Biol.*
585 *Assoc. United Kingdom* 22, 469–484.
- 586 Cole, H.A., 1937. Metamorphosis of the larva of *Ostrea edulis*. *Nature* 139, 413.
- 587 Cury, P., Roy, C., 1989. Optimal environmental window and pelagic fish recruitment success in
588 upwelling areas. *Can. J. Fish. Aquat. Sci.* 46, 670–680.
- 589 Doroudi, M.S., Southgate, P.C., 2003. Embryonic and larval development of *Pinctada margaritifera*
590 (Linnaeus, 1758). *Molluscan Res.* 23, 101–107.
- 591 Doroudi, M.S., Southgate, P.C., 2000. The influence of algal ration and larval density on growth and
592 survival of blacklip pearl oyster *Pinctada margaritifera* (L.) larvae. *Aquac. Res.* 31, 621–626.
- 593 Doroudi, M.S., Southgate, P.C., Lucas, J.S., 2003. Variation in clearance and ingestion rates by larvae
594 of the blacklip pearl oyster (*Pinctada margaritifera*, L.) feeding on various microalgae. *Aquac.*
595 *Nutr.* 9, 11–16.
- 596 Doroudi, M.S., Southgate, P.C., Mayer, R.J., 1999. The combined effects of temperature and salinity
597 on embryos and larvae of the blacklip pearl oyster, *Pinctada margaritifera* (L.). *Aquac. Res.* 30,
598 271–277.
- 599 Doroudi, M.S., Southgate, P.C., Mayer, R.J., 1999. Growth and survival of blacklip pearl oyster larvae
600 fed different densities of microalgae. *Aquac. Int.* 7, 179–187.
- 601 Ehteshami, F., Christianus, A., Rameshi, H., Harmin, S.A., Saad, C.R., 2011. The effects of dietary
602 supplements of polyunsaturated fatty acid on pearl oyster, *Pinctada margaritifera* L., gonad
603 composition and reproductive output. *Aquac. Res.* 42, 613–622.
- 604 Fournier, J., 2011. Alimentation et déterminisme environnemental de la reproduction des huîtres
605 perlières *P. margaritifera* sur l'atoll d'Ahe (Archipel des Tuamotu, Polynésie française), Diet and
606 environmental determinism of reproduction of pearl oysters *P. margaritifera* on A.
- 607 Fournier, J., Dupuy, C., Bouvy, M., Couraudon-Réale, M., Charpy, L., Pouvreau, S., Le Moullac, G., Le
608 Pennec, M., Cochard, J.-C., 2012. Pearl oysters *Pinctada margaritifera* grazing on natural

609 plankton in Ahe atoll lagoon (Tuamotu archipelago, French Polynesia). *Mar. Pollut. Bull.* 65, 490–
610 499.

611 Fox, J., Weisberg, S., Adler, D., Bates, D., Baud-Bovy, G., Ellison, S., Firth, D., Friendly, M., Gorjanc,
612 G., Graves, S., 2012. Package ‘car.’ Vienna R Found. Stat. Comput.

613 Gerdes, D., 1983. The Pacific oyster *Crassostrea gigas*: Part II. Oxygen consumption of larvae and
614 adults. *Aquaculture* 31, 221–231.

615 Gnaiger, E., 1983. Heat dissipation and energetic efficiency in animal anoxibiosis: economy contra
616 power. *J. Exp. Zool.* 228, 471–490.

617 González-Araya, R., Quéau, I., Quéré, C., Moal, J., Robert, R., 2011. A physiological and
618 biochemical approach to selecting the ideal diet for *Ostrea edulis* (L.) broodstock conditioning
619 (part A). *Aquac. Res.* 42, 710–726.

620 Grosberg, R.K., Levitan, D.R., 1992. For adults only? Supply-side ecology and the history of larval
621 biology. *Trends Ecol. Evol.* 7, 130–133.

622 Hamburger, K., Møhlenberg, F., Randløv, A., Riisgård, H.U., 1983. Size, oxygen consumption and
623 growth in the mussel *Mytilus edulis*. *Mar. Biol.* 75, 303–306.

624 Hjort, J., 1926. Fluctuations in the year classes of important food fishes. *ICES J. Mar. Sci.* 1, 5–38.

625 Hofmann, E., Bushek, D., Ford, S., Guo, X., Haidvogel, D., Hedgecock, D., Klinck, J., Milbury, C.,
626 Narvaez, D., Powell, E., Wang, Y., Wang, Z., Wilkin, J., Zhang, L., 2009. Understanding how
627 disease and environment combine to structure resistance in estuarine bivalve populations.
628 *Oceanography* 22, 212–231.

629 Holland, D.L., Spencer, B.E., 1973. Biochemical changes in fed and starved oysters, *Ostrea edulis* L.
630 during larval development, metamorphosis and early spat growth. *J. Mar. Biol. Assoc. United*
631 *Kingdom* 53, 287–298.

632 Hothorn, T., Bretz, F., Westfall, P., Heiberger, R.M., Schuetzenmeister, A., Scheibe, S., Hothorn, M.T.,
633 2017. Package ‘multcomp.’ Obtenido de [http://cran. statsfu.](http://cran.r-project.org/web/packages/multcomp/multcomp)
634 [ca/web/packages/multcomp/multcomp](http://cran.r-project.org/web/packages/multcomp/multcomp).

635 ISPF, 2016. Le bilan de la perles en 2016. [WWW Document].

636 Jager, T., Vandenbrouck, T., Baas, J., De Coen, W.M., Kooijman, S.A.L.M., 2010. A biology-based
637 approach for mixture toxicity of multiple endpoints over the life cycle. *Ecotoxicology* 19, 351–361.

638 Jager, T., Zimmer, E.I., 2012. Simplified dynamic energy budget model for analysing ecotoxicity data.
639 *Ecol. Modell.* 225, 74–81.

640 Kooijman, S., 2010. *Dynamic energy budget theory for metabolic organisation*. Cambridge university
641 press.

642 Lenth, R. V, 2016. Least-squares means: the R package lsmeans. *J. Stat. Softw.* 69, 1–33.

643 Lika, K., Kearney, M.R., Freitas, V., van der Veer, H.W., van der Meer, J., Wijsman, J.W.M.,
644 Pecquerie, L., Kooijman, S.A.L.M., 2011. The “covariation method” for estimating the parameters
645 of the standard Dynamic Energy Budget model I: Philosophy and approach. *J. Sea Res.* 66,
646 270–277.

647 Lüdecke, M.D., 2015. Package ‘sjPlot.’

648 Marshall, D.J., Styan, C., McQuaid, C.D., 2009. Larval supply and dispersal, in: *Marine Hard Bottom*

649 Communities. Springer, pp. 165–176.

650 Menge, B.A., Chan, F., Nielsen, K.J., Lorenzo, E. Di, Lubchenco, J., 2009. Climatic variation alters
651 supply-side ecology: impact of climate patterns on phytoplankton and mussel recruitment. *Ecol.*
652 *Monogr.* 79, 379–395.

653 Moran, A.L., Manahan, D.T., 2004. Physiological recovery from prolonged ‘starvation’ in larvae of the
654 Pacific oyster *Crassostrea gigas*. *J. Exp. Mar. Bio. Ecol.* 306, 17–36.

655 O’Connor, M.I., Bruno, J.F., Gaines, S.D., Halpern, B.S., Lester, S.E., Kinlan, B.P., Weiss, J.M., 2007.
656 Temperature control of larval dispersal and the implications for marine ecology, evolution, and
657 conservation. *Proc. Natl. Acad. Sci.* 104, 1266–1271.

658 Olson, R.R., Olson, M.H., 1989. Food limitation of planktotrophic marine invertebrate larvae: does it
659 control recruitment success? *Annu. Rev. Ecol. Syst.* 20, 225–247.

660 Pagano, M., Rodier, M., Guillaumot, C., Thomas, Y., Henry, K., Andréfouët, S., 2017. Ocean-lagoon
661 water and plankton exchanges in a semi-closed pearl farming atoll lagoon (Ahe, Tuamotu
662 archipelago, French Polynesia). *Estuar. Coast. Shelf Sci.* 191, 60–73.

663 Pechenik, J.A., 1990. Delayed metamorphosis by larvae of benthic marine invertebrates: does it
664 occur? Is there a price to pay? *Ophelia* 32, 63–94.

665 Pouvreau, S., Bodoy, A., Buestel, D., 2000. In situ suspension feeding behaviour of the pearl oyster,
666 *Pinctada margaritifera*: combined effects of body size and weather-related seston composition.
667 *Aquaculture* 181, 91–113.

668 Pouvreau, S., Bourles, Y., Lefebvre, S., Gangnery, A., Alunno-Bruscia, M., 2006. Application of a
669 dynamic energy budget model to the Pacific oyster, *Crassostrea gigas*, reared under various
670 environmental conditions. *J. Sea Res.* 56, 156–167.

671 Pouvreau, S., Prasil, V., 2001. Growth of the black-lip pearl oyster, *Pinctada margaritifera*, at nine
672 culture sites of French Polynesia: synthesis of several sampling designs conducted between
673 1994 and 1999. *Aquat. Living Resour.* 14, 155–163.

674 Pouvreau, S., Tiapari, J., Gangnery, A., Lagarde, F., Garnier, M., Teissier, H., Haumani, G., Buestel,
675 D., Bodoy, A., 2000. Growth of the black-lip pearl oyster, *Pinctada margaritifera*, in suspended
676 culture under hydrobiological conditions of Takapoto lagoon (French Polynesia). *Aquaculture*
677 184, 133–154.

678 Powell, E.N., Bochenek, E.A., Klinck, J.M., Hofmann, E.E., 2002. Influence of food quality and quantity
679 on the growth and development of *Crassostrea gigas* larvae: a modeling approach. *Aquaculture*
680 210, 89–117.

681 Rico-Villa, B., Bernard, I., Robert, R., Pouvreau, S., 2010. A Dynamic Energy Budget (DEB) growth
682 model for Pacific oyster larvae, *Crassostrea gigas*. *Aquaculture* 305, 84–94.

683 Rico-Villa, B., Pouvreau, S., Robert, R., 2009. Influence of food density and temperature on ingestion,
684 growth and settlement of Pacific oyster larvae, *Crassostrea gigas*. *Aquaculture* 287, 395–401.

685 Ripley, B., Venables, B., Bates, D.M., Hornik, K., Gebhardt, A., Firth, D., Ripley, M.B., 2013. Package
686 ‘mass.’ CRAN Repos. [Httpcran R-Proj. OrgwebpackagesMASSMASS Pdf.](http://cran.R-Project.org/web/packages/MASS/MASS.Pdf)

687 Southgate, P., Lucas, J., 2011. *The pearl oyster*. Elsevier.

688 Strugnell, J.M., Southgate, P.C., 2003. Changes in tissue composition during larval development of

689 the blacklip pearl oyster, *Pinctada margaritifera* (L.). *Molluscan Res.* 23, 179–183.

690 Thomas, Y., Dumas, F., Andréfouët, S., 2016. Larval connectivity of pearl oyster through biophysical
691 modelling; evidence of food limitation and broodstock effect. *Estuar. Coast. Shelf Sci.* 182, 283–
692 293.

693 Thomas, Y., Garen, P., Bennett, A., Le Pennec, M., Clavier, J., 2012. Multi-scale distribution and
694 dynamics of bivalve larvae in a deep atoll lagoon (Ahe, French Polynesia). *Mar. Pollut. Bull.* 65,
695 453–462.

696 Thomas, Y., Garen, P., Courties, C., Charpy, L., 2010. Spatial and temporal variability of the pico-and
697 nanophytoplankton and bacterioplankton in a deep Polynesian atoll lagoon. *Aquat. Microb. Ecol.*
698 59, 89–101.

699 Thomas, Y., Garen, P., Pouvreau, S., 2011. Application of a bioenergetic growth model to larvae of the
700 pearl oyster *Pinctada margaritifera* L. *J. sea Res.* 66, 331–339.

701 Thorson, G., 1950. Reproductive and larval ecology of marine bottom invertebrates. *Biol. Rev.* 25, 1–
702 45.

703 Underwood, A.J., Fairweather, P.G., 1989. Supply-side ecology and benthic marine assemblages.
704 *Trends Ecol. Evol.* 4, 16–20.

705 Wickham, H., 2010. *ggplot2: elegant graphics for data analysis.* J Stat Softw.

706 Widdows, J., 1991. Physiological ecology of mussel larvae. *Aquaculture* 94, 147–163.

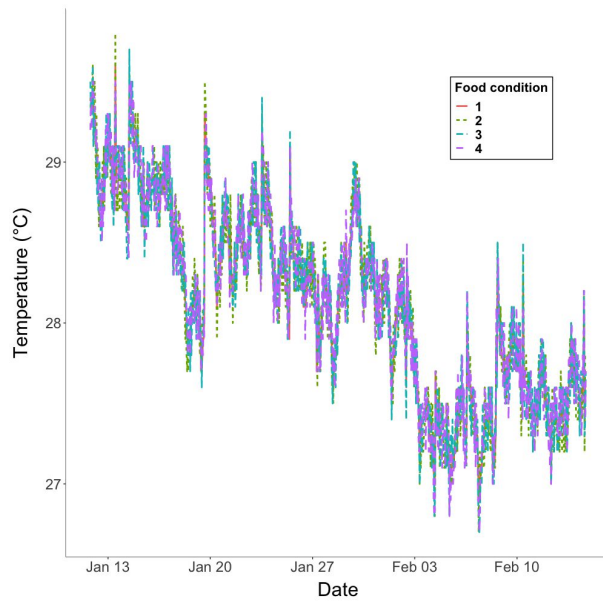
707 Yukihiro, H., Lucas, J.S., Klumpp, D.W., 2000. Comparative effects of temperature on suspension
708 feeding and energy budgets of the pearl oysters *Pinctada margaritifera* and *P. maxima*. *Mar.*
709 *Ecol. Prog. Ser.* 195, 179–188.

710

711

712 **Supplementary material**

713



714

715 **Figure 1: Temperature profiles across time for each feeding condition**

716